PAPER

Check for updates

An *in situ* DRIFTS study on nitrogen electrochemical reduction over an Fe/BaZr$_{0.8}$Y$_{0.2}$O$_{3-\delta}$-Ru catalyst at 220 °C in an electrolysis cell using a CsH$_2$PO$_4$/SiP$_2$O$_7$ electrolyte

Yao Yuan,[a] Naoya Fujiwara,[a] Shohei Tada [b] and Ryuji Kikuchi [*a]

In situ DRIFTS measurements of an Fe/BZY-Ru cathode catalyst in an electrolysis cell using a CsH$_2$PO$_4$/SiP$_2$O$_7$ electrolyte were carried out in a mixed N$_2$–H$_2$ gas flow under polarization. The formation of N$_2$H$_x$ species was confirmed under polarization, and an associative mechanism in the electrochemical NRR process was verified.

NH$_3$ production contributes about 2% of the world's energy consumption annually, and most of the consumption is from the strongly endothermic steam reforming of methane (SRM) at 800–1000 °C in the Haber–Bosch process. Other major energy consuming processes include CO$_2$ removal, reactant gas purification, reactant gas compression for NH$_3$ synthesis, and NH$_3$ separation.[1] Due to its high energy density, NH$_3$ was expected to be a promising energy carrier in recent years.[2] NH$_3$ produced by renewable energy sources can be used as a carbon-free energy carrier. One of the promising methods to utilize renewable energy sources for NH$_3$ production is electrochemical N$_2$ reduction. Various electrolysis cells with solid and liquid electrolytes have been reported for electrochemical N$_2$ reduction over a wide temperature range. For the electrochemical N$_2$ reduction reaction (NRR) at low temperatures ($T < 100$ °C), the main limitation is the difficulty of N$_2$ activation and the low solubility of N$_2$ in aqueous media. High temperatures ($T > 500$ °C) can lead to decomposition of the produced NH$_3$. Hence, an electrochemical NRR at intermediate temperatures is desirable. Phosphates such as CsH$_2$PO$_4$ and CsH$_5$(PO$_4$)$_2$ are typically used as electrolytes at intermediate temperatures. These inorganic oxyacid salts have high proton conductivity and stability. CsH$_2$PO$_4$ mixed with SiP$_2$O$_7$ as a matrix exhibits a proton conductivity of *ca.* 1×10^{-2} S cm^{-1} at 220 °C.[3] In our previous work on electrochemical NH$_3$ synthesis using an Fe/BZY-RuO$_2$ catalyst and CsH$_2$PO$_4$/SiP$_2$O$_7$ electrolyte at 220 °C and ambient pressure, the highest current efficiency of 7.1% and the highest NH$_3$ yield rate of 4.5×10^{-10} mol (s^{-1} cm^2) were achieved at −0.4 V (*vs.* open circuit voltage (OCV)) and −1.5 V, respectively. In addition, N$_2$H$_4$ was successfully detected at −0.2 V (*vs.* OCV),

which indicated an associative mechanism,[4] which is one of the two main reaction mechanisms in NH$_3$ synthesis, namely, associative and dissociative mechanisms. In the associative mechanism the N≡N bond in a N$_2$ molecule adsorbed on the catalyst surface is cleaved after an H atom attaches to the N atom of the adsorbed N$_2$ molecule, whereas in the dissociative mechanism the N≡N bond is broken on the catalyst surface before an H atom attaches to the N$_2$ molecule.

Typical electrochemical characterizations such as impedance spectroscopy,[5,6] current–voltage curve (*IV* curve) testing,[7,8] cyclic voltammetry,[9] and potentiostatic pulse experiment[10] can only provide indirect information on surface reactions at the electrode. It is indispensable to analyse directly adsorbed species on the electrode catalysts for the understanding of the reaction mechanism. *In situ* spectroscopy is making rapid progress and has already been applied to electrochemical devices, providing valuable information of the chemical species during the reactions.[11] *In situ* diffuse reflectance infrared Fourier transform spectroscopy (DRIFTS) for electrolysis cells attracts much attention recently.[12,13] *In situ* DRIFTS has recently become a powerful tool for investigating the reaction pathway in electrochemical N$_2$ reduction reaction.[14–16] In DRIFTS, infrared (IR) beam irradiates the sample disk, and then can be reflected at or transmitted through the sample disk. The scattered IR beam is collected by the spherical focusing mirrors and finally converted by a detector.

In this work, a commercial DRIFTS setup was modified and applied to electrochemical N$_2$ reduction as shown in Fig. 1. To enable an operation temperature higher than 200 °C that is requisite for proton conduction in the electrolyte, an electrical heating wire was placed in the base near the micro-cup. The temperature was measured by a thermocouple located next to the heating wire. An electrolysis cell was set on the micro-cup of the metal base. For protection of the ZnSe window from oxidation at the high operating temperature, a water-cooling

a Department of Chemical System Engineering, The University of Tokyo, 7-3-1, Hongo, Bunkyo-ku, Tokyo 113-8656, Japan. E-mail: rkikuchi@chemsys.t.u-tokyo.ac.jp
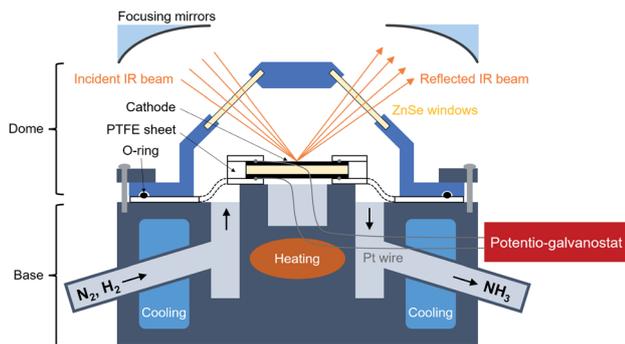*b Department of Materials Sciences and Engineering, Ibaraki University, Ibaraki, 316-8511, Japan*

Fig. 1 A schematic of modified DRIFTS setup applied to electrochemical N_2 reduction. The temperature of the electrolysis cell is measured at the same place where it is heated.

Fig. 3 A schematic of electrolysis cell on the micro-cup.

system was attached to the metal base near the dome to keep the temperature of the window below 200 °C. The specific size of the apparatus is shown in the Fig. 2. An O-ring fits to the dome can ensure gas tightness of the small space in the dome. There are three pathways which connect the inside space of the dome and atmosphere. Two of them are used for the inlet and outlet gas flows, and the one connecting directly with the micro-cup was used for Pt lead wires. To avoid a short-circuit between the two Pt lead wires, a thin polyimide film (12.5 μm thick, Kapton, Dupont, Delaware, United States) which is stable from −269 to +400 °C was used to cover the Pt wires.

In our previous study of the electrochemical NH_3 synthesis process at 220 °C, a ⌀ 10 mm carbon paper was used on the cathode side to increase the current collection area.[4] However, in the *in situ* DRIFTS tests, the cathode catalysts must be exposed to the IR beam, hence a carbon ring with an inside diameter of 7 mm was used instead as shown in Fig. 3. On the anode side, a ⌀ 10 mm Pt/C loaded on carbon paper was used for current collection. The electrolysis cell consists of 0.1 g SiP_2O_7/CsH_2PO_4 electrolyte (mix ratio of $SiP_2O_7 : CsH_2PO_4$ was 1 : 1) compressed with 0.035 g Fe/BZY-Ru (mix ratio of Fe/BZY : RuO_2 was 1 : 1) catalyst on the top layer. In our previous work of the electrochemical NH_3 synthesis using Fe/BZY-RuO_2, we have successfully detected N_2H_4 as well as NH_3, which indicated the triple bond of N_2 was broken simultaneously with the addition of H. Fe/BZY was prepared in the same way
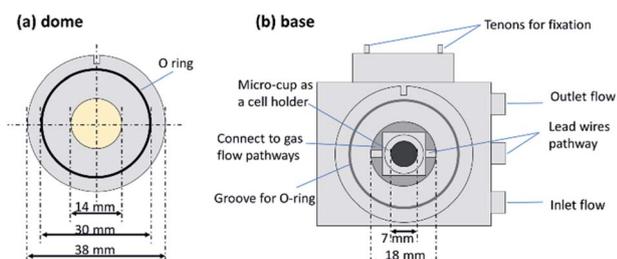
as in the previous work.[4] The as-prepared Fe/BZY powder was mixed with RuO_2 powder, and then the mixture was reduced in H_2 flow at 220 °C for 1 h. To fix the electrolysis cell, the current collection materials and the Pt lead wires, PTFE sheets (Gore Hyper-Sheet Gasket, W. L. Gore & Associate, Inc., Delaware, USA) formed into rings were used as the support. The experimental conditions in the dome are similar to those in a single-chamber reactor. The inlet gas is a mixture of N_2 and H_2, which is different from the two-chamber reactor in electrolysis tests in the previous work. A background spectrum was measured under H_2 gas flow of 8 mL min^{-1} at 160 °C with 100 scans at OCV. All DRIFTS spectra are displayed as $\log(I_0/I)$ where I_0/I is the relative reflectance (I_0 is the background reflectance). Then the measurements were carried out under N_2 gas flow of 8 mL min^{-1} at 300 °C at OCV and under mixed N_2 and H_2 gas flow (both are 8 mL min^{-1}) at 250 °C at OCV and various applied biases.

According to the results in Fig. 4, three kinds of sharp peaks at 1050, 1300 and 1540 cm^{-1}, and a broad peak at 3300 cm^{-1} were observed. Peak at 1050 cm^{-1} is attributed to N–N stretching (reported at 1106 cm^{-1}),[17] which appeared in all experimental conditions even when only N_2 gas was supplied.

Fig. 2 (a) The bottom-up view of the dome. (b) The vertical view of the metal base.

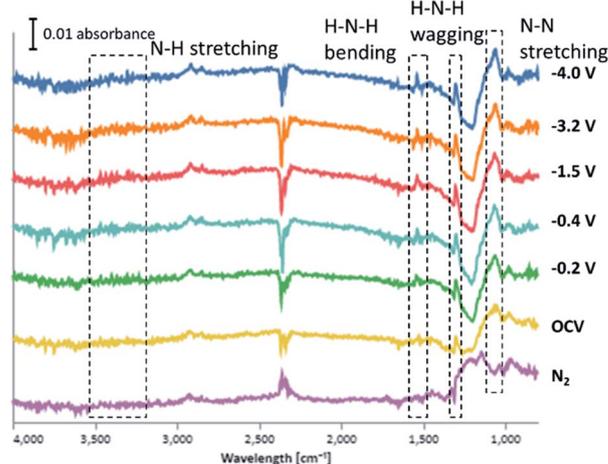Fig. 4 Electrochemical *in situ*-FTIR spectra of the NRR on the Fe/BZY-Ru electrode at various electrochemical potentials. Then the measurements were carried out under N_2 at 300 °C at OCV and under mixed N_2 and H_2 at 250 °C at OCV, −0.2, −0.4, −1.5, −3.2 and −4.0 V.
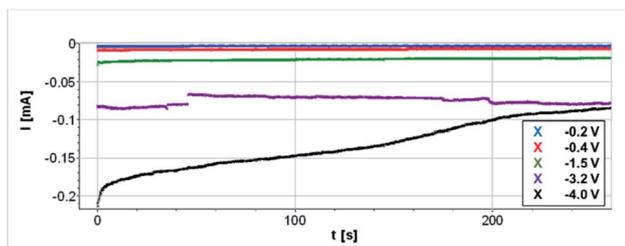
Fig. 5 Currents for applied voltages of −0.2 V, −0.4 V, −1.5 V, −3.2 V, and −4.0 V.

This implies that the N_2 adsorption sites on the catalyst surface are highly active. Peaks at 1300, 1540 and 3300 cm^{-1} are assigned to H–N–H wagging, H–N–H bending and N–H stretching (reported at 1270, 1461 and 3235 cm^{-1}).[17] These three kinds of peaks appeared only when both N_2 and H_2 were supplied, and seem to become stronger with applied bias. It is obvious that N_2H_x species, which can be intermediate species in the associative mechanism, were formed on the surface of Fe/BZY-Ru. The peak at 900 cm^{-1} is probably attributed to NH_3 gas.[18] It is likely that the peaks at 1400 cm^{-1} and 2800 cm^{-1} are assigned to NH_4^+.[19] The strong signal at 2360 cm^{-1} is associative with gas-phase CO_2 that exists in IR beam path outside the dome.

Only quite low current densities were able to be loaded as shown in Fig. 5. Reactant gases were introduced to the system without humidification, which might have led to low proton conductivity and electrolyte decomposition. In addition, current collection area of the carbon paper ring on the cathode side is small.

In situ DRIFTS measurements were carried out in a N_2–H_2 gas mixture under polarization, which corresponds to a situation in a single-chamber reactor. The background was measured in H_2 flow, and the sample measurements were carried out in a mixed N_2–H_2 gas flow. In the obtained spectra, a peak at 1100 cm^{-1} was assigned to N–N stretching, and those at 1301, 1600, and 3300 cm^{-1} were assigned to –NH_2 wagging, H–N–H bending, and N–H stretching. The intensity of the H–N–H wagging peak was enhanced by increasing the applied voltage. Appearance of these peaks confirmed the formation of N_2H_x ($1 \leq x \leq 4$) species in the NRR process and consequently demonstrated that NRR proceeded *via* an associative mechanism over Fe/BZY-Ru cathode catalyst on a SiP_2O_7/CsH_2PO_4 electrolyte.

Author contributions

Yao Yuan: investigation, data curation, formal analysis, writing – original draft. Naoya Fujiwara: methodology, resources, visualization. Shohei Tada: methodology, data curation, formal analysis. Ryuji Kikuchi: conceptualization, supervision, writing – review & editing.

Conflicts of interest

There are no conflicts to declare.

Acknowledgements

References

1 I. Rafiqul, C. Weber, B. Lehmann and A. Voss, *Energy*, 2005, **30**, 2487–2504.

2 N. V. Rees and R. G. Compton, *Energy Environ. Sci.*, 2011, **4**, 1255–1260.

3 N. Fujiwara, H. Nagase, S. Tada and R. Kikuchi, *ChemSusChem*, 2021, **14**, 417–427.

4 Y. Yuan, S. Tada and R. Kikuchi, *Mater. Adv.*, 2021, **2**, 793–803.

5 R. Lan and S. Tao, *RSC Adv.*, 2013, **3**, 18016–18021.

6 B. Xu, L. Xia, F. Zhou, R. Zhao, H. Chen, T. Wang, Q. Zhou, Q. Liu, G. Cui, X. Xiong, F. Gong and X. Sun, *ACS Sustainable Chem. Eng.*, 2019, **7**, 2889–2893.

7 P. Shen, Y. Liu, Q. Li and K. Chu, *Chem. Commun.*, 2020, **56**, 10505–10508.

8 Q. Fan, C. Choi, C. Yan, Y. Liu, J. Qiu, S. Hong, Y. Jung and Z. Sun, *Chem. Commun.*, 2019, **55**, 4246–4249.

9 K. Fricke, F. Harnisch and U. Schröder, *Energy Environ. Sci.*, 2008, **1**, 144–147.

10 Y. Jännsch, J. J. Leung, M. Hämmerle, E. Magori, K. Wiesner-Fleischer, E. Simon, M. Fleischer and R. Moos, *Electrochem. Commun.*, 2020, **121**, 106861.

11 M. F. Baruch, J. E. Pander, J. L. White and A. B. Bocarsly, *ACS Catal.*, 2015, **5**, 3148–3156.

12 D. J. Cumming, C. Tumilson, S. F. R. Taylor, S. Chansai, A. V. Call, J. Jacquemin, C. Hardacre and R. H. Elder, *Faraday Discuss.*, 2015, **182**, 97–111.

13 N. Shi, Y. Xie, D. Huan, Y. Yang, S. Xue, Z. Qi, Y. Pan, R. Peng, C. Xia and Y. Lu, *J. Mater. Chem. A*, 2019, **7**, 4855–4864.

14 Y. Yao, S. Zhu, H. Wang, H. Li and M. Shao, *J. Am. Chem. Soc.*, 2018, **140**, 1496–1501.

15 X. Qu, L. Shen, Y. Mao, J. Lin, Y. Li, G. Li, Y. Zhang, Y. Jiang and S. Sun, *ACS Appl. Mater. Interfaces*, 2019, **11**, 31869–31877.

16 J.-T. Ren, C.-Y. Wan, T.-Y. Pei, X.-W. Lv and Z.-Y. Yuan, *Appl. Catal., B*, 2020, **266**, 118633.

17 P. Song, H. Wang, L. Kang, B. Ran, H. Song and R. Wang, *Chem. Commun.*, 2019, **55**, 687–690.

18 S. Süzer and L. Andrews, *J. Chem. Phys.*, 1987, **87**, 5131–5140.

19 C. Sun and D. Xue, *CrystEngComm*, 2015, **17**, 2728–2736.